

Site-Directed Mutants of Rat Testis Fructose 6-Phosphate, 2-Kinase/Fructose 2,6-Bisphosphatase: Localization of Conformational Alterations Induced by Ligand Binding[†]

Michael K. Helms,[‡] Theodore L. Hazlett,[§] Hiroyuki Mizuguchi,^{||} Charles A. Hasemann,[⊥] Kosaku Uyeda,^{||} and David M. Jameson^{*:‡}

Department of Genetics and Molecular Biology, University of Hawaii at Manoa, 1960 East-West Road, Honolulu, Hawaii 96822, Laboratory for Fluorescence Dynamics, Physics Department, University of Illinois at Urbana—Champaign, 1110 West Green Street, Urbana, Illinois 61801, Research Service, Department of Veterans Affairs Medical Center, Biochemistry Department and Internal Medicine, University of Texas Southwestern Medical Center at Dallas, Dallas, Texas 75216, and Department of Internal Medicine, University of Texas Southwestern Medical Center, 5323 Harry Hines Boulevard, Dallas, Texas 75235

Received January 27, 1998; Revised Manuscript Received June 15, 1998

ABSTRACT: Site-directed mutagenesis was utilized to construct mutants, containing one or two tryptophan residues, of the bifunctional enzyme fructose 6-phosphate,2-kinase–fructose 2,6-bisphosphatase. Two of the single-tryptophan mutants (W15 and W64) had the tryptophan residue located in the kinase domain, which is in the N-terminal half, and two (W299 and W320) had the tryptophan residue located in the phosphatase domain, which is in the C-terminal half. The double-tryptophan mutants were W15/W64, W15/W299, W64/W299, and W299/W320. Dynamic polarization data indicated that these tryptophan residues had varying degrees of local mobility. Steady-state polarization data revealed energy transfer between the tryptophan residues in the double mutant W299/W320 but not in the W15/W64, W15/W299, or W64/W299 mutants, indicating the proximity of the W299 and W320 residues. The binding of fructose-6-phosphate resulted in a significant increase in the anisotropy of the W15 mutants, but did not affect the anisotropies of any of the other single-tryptophan mutants. Binding of fructose-2,6-bisphosphate also significantly increased the anisotropy of W15. In the case of fructose-6-phosphate binding, the increased anisotropy was shown to be due to a restriction of the tryptophan residue's local mobility in the presence of bound ligand, which suggests that the N-terminus is located near the kinase active site. These increases in anisotropies were used to estimate the dissociation constants of fructose-6-phosphate and fructose-2,6-bisphosphate, which were 29 ± 3 and $2.1 \pm 0.3 \mu\text{M}$, respectively. These observations are considered in light of the recently published crystal structure for this bifunctional enzyme.

Fructose 6-phosphate,2-kinase/fructose 2,6-bisphosphatase (F6P,2-kinase/F2,6-Pase)¹ is a bifunctional enzyme which catalyzes the synthesis and degradation of Fru 2,6-P₂, a potent activator of phosphofructokinase, one of the key regulatory enzymes of glycolysis. Several tissue-specific isozymes of F6P,2-kinase/F2,6-Pase have been isolated and characterized (reviewed in ref 1). These isozymes, which are homodimers composed of subunits with molecular weights ranging from 54 to 60 kDa, have different relative kinase and phosphatase

activities. The kinase activity resides in the N-terminal half of the enzyme while the phosphatase activity is located in the C-terminal half. Although the amino acid sequences of the catalytic domains of all known isozymes are well-conserved, the extreme N- and C-terminal peptides differ significantly and presumably confer the differences in the relative kinase and phosphatase activities (2–7). Phosphorylation and dephosphorylation of the enzyme can regulate the relative ratios of the kinase and phosphatase activities. For example, phosphorylation of the N-terminus of the liver enzyme activates its phosphatase activity but inhibits its kinase activity (8–10). Phosphorylation of the C-terminus of the heart enzyme, however, activates the kinase activity while leaving the phosphatase activity unchanged (11, 12).

The wild-type enzyme (from rat testis) contains four tryptophan residues, namely W15, W64, W299, and W320. The crystal structure of a mutant form of rat testis Fru-6-P,2-kinase/Fru-2,6-Pase, in which all four of the tryptophan residues have been altered to phenylalanine, was recently solved (13). These substitutions do not significantly alter the kinetic and physical properties of the enzyme (14). The structure revealed that residue 64 is located in the interdomain

[†] This work was supported in part by grants from the Department of Veterans Affairs (K.U.), the NIDDK (DK16194) (K.U.), the Welch Foundation (I-1318) (C.A.H.), the American Heart Association, Texas Affiliate (96G-098) (C.A.H.), and the National Science Foundation (MCB-9506845) (D.M.J.).

* To whom correspondence should be addressed.

[‡] University of Hawaii at Manoa.

[§] University of Illinois at Urbana—Champaign.

^{||} Department of Veterans Affairs Medical Center, University of Texas Southwestern Medical Center at Dallas.

[⊥] Department of Internal Medicine, University of Texas Southwestern Medical Center.

¹ Abbreviations: Fru 6-P,2-kinase/Fru 2,6-Pase, fructose 6-phosphate,2-kinase/fructose 2,6-bisphosphatase; Fru-6-P, fructose-6-phosphate; Fru-2,6-P₂, fructose-2,6-bisphosphate.

region of the enzyme, while residues 299 and 320 are in close proximity to each other in the phosphatase domain. The N-terminal 36 residues were disordered in the crystal, suggesting that the N-terminus may be highly mobile. Although a 3-D structure of an ATP-bound form of the testis enzyme has been solved (13), conformation of the enzyme with and without bound ligands has not been elucidated.

To gain insight into the roles of the N-terminal peptide, we previously prepared mutants with 24–30 amino acids deleted from the N-terminus of the testis enzyme (15). These deletions caused a large increase in K_M for Fru-6-P, a decrease in Fru-6-P,2-kinase activity, and an increase in Fru-2,6-bisphosphatase activity. Furthermore, the deletion mutants were more susceptible to dissociation and thermal inactivation. A similar effect on Fru-6-P binding and on the kinetic properties of N-terminus deletion mutants was reported for the liver isozyme (16). These results suggest that the N-terminus is important in stabilization of the dimeric structure and is involved in Fru-6-P binding and catalysis. However, structural details of the interaction of the N-terminus with the catalytic domains are not available.

The approach using site-directed mutagenesis to incorporate or remove tryptophan residues in proteins and to study the variants using fluorescence methodologies has become a widely used experimental stratagem (for recent examples see refs 17–24). Hence, to investigate the conformational dynamics of F6P,2-kinase:F2,6-Pase in general, and in the N-terminus region in particular, we constructed the four single-tryptophan-containing mutants (14), thus placing probes in specific locations in the protein matrix. The enzymatic and steady-state fluorescence properties of these single-tryptophan-containing mutants were then used to follow the unfolding and refolding of these proteins in guanidinium chloride (14). The polarization of each tryptophan residue was also measured, and it was found that the wild-type enzyme had a significantly lower polarization than any of the single-tryptophan residues, suggesting that energy transfer leading to depolarization occurs between two or more of the tryptophan residues (14). In this study, we present time-resolved fluorescence results aimed at elucidating the mobilities of each tryptophan residue in the absence and presence of the physiological substrates, fructose 6-phosphate and fructose 2,6-bisphosphate. We also constructed and studied several double-tryptophan variants to investigate the possibility of nonradiative energy transfer between tryptophan residues. All of our fluorescence studies were designed to provide information on dynamic aspects of the protein to augment the structural studies and to investigate the region near the W15 residue, which was not resolved in the crystallographic structure.

MATERIALS AND METHODS

Homogeneous recombinant rat testis Fru-6-P,2-kinase/Fru-2,6-bisphosphatase and the mutant enzymes described were prepared from *Escherichia coli* BL21(DE3) carrying appropriate genes as previously described (15). Restriction enzymes and bacteriophage T4 DNA ligase were purchased from New England Biolabs (Beverly, MA) and Pharmacia LKB Biotechnology, Inc. (Piscataway, NJ). A MutaGene M13 in vitro mutagenesis kit was purchased from Bio Rad Laboratories (Richmond, CA). All other chemicals were reagent grade and obtained from commercial sources.

Construction of single-tryptophan mutant plasmids, W15/pT7-7, W64/pT7-7, W299/pT7-7, and W320/pT7-7, was as previously described (14). Double-tryptophan mutant plasmids, W15W64/pT7-7, and W299W320/pT7-7, were also constructed as previously described (14). W15/W299 and W64/W320 double-mutant plasmids were constructed using the single-tryptophan mutant plasmids as follows. W299/pT7-7 DNA was digested with *SacI* and *HindIII*, and the resulting 0.9 kb DNA fragment containing W299 was isolated. This fragment was ligated into the *SacI/HindIII* site of the W15/pT7-7 plasmid. The corresponding procedure was followed to produce the other double-tryptophan mutants.

Protein concentration was determined by the method of Bradford (25) using bovine serum albumin as a standard. Previously, we found that the extinction coefficient of the colored product based on the dry weight of the pure enzyme was identical to that of bovine serum albumin (26). The buffer used contained 50 mM Tris-Cl, pH 7.5, 5 mM DTT, and 1 mM $MgCl_2$.

Time-resolved fluorescence experiments were performed at the Laboratory for Fluorescence Dynamics (LFD) at the University of Illinois, Urbana–Champaign, using a multi-frequency phase and modulation fluorometer. In the instrument utilized, the frequency modulation of the excitation source is realized using the harmonic content approach (27, 28). The exciting light was from a Coherent Nd:YAG mode-locked laser pumping a rhodamine dye laser. The dye laser was tuned to 600 nm, which was then frequency doubled to 300 nm. Emission was observed through a Corning 7-54 broad band-pass filter and a Schott WG-335 filter to isolate the tryptophan emission (at $\lambda > 330$ nm) and block scattered light. The exciting light was polarized parallel to the vertical laboratory axis, and the emission was viewed through a polarizer oriented at 55° (29). Phase and modulation values for both lifetime and dynamic polarization data were obtained as previously described (30–32). The lifetime data were analyzed either by assuming a sum of discrete exponentials (31) or by using continuous distribution models which assumed either Lorentzian or Gaussian distributions (33–35), and the goodness of fit of the data to a particular model was judged by the value of the reduced chi-square (χ^2). Globals Unlimited software (Urbana, IL) was used for analyses which was performed using a constant, frequency-independent standard deviation of 0.2° for phase and 0.004 for modulation. Correlated error analyses (i.e., one parameter is varied near the χ^2 minimum while the other parameters are all free) were performed on the lifetimes and rotational correlation times, and the rigorous 67% confidence limits are reported for each parameter.

The multifrequency phase and modulation method also permits characterization of the rotational modes of fluorophores using differential polarized phase fluorometry, also known as dynamic polarization. In this approach, the exciting light, modulated at varying frequencies, is polarized parallel to the laboratory axis, and the phase delay between the perpendicular and parallel components of the emission is determined as well as the ratio of their AC components. The theoretical expressions describing the dynamic polarization data, which is the frequency domain equivalent of anisotropy decay, are more easily apprehended when written in the time domain. Specifically, the time-resolved anisot-

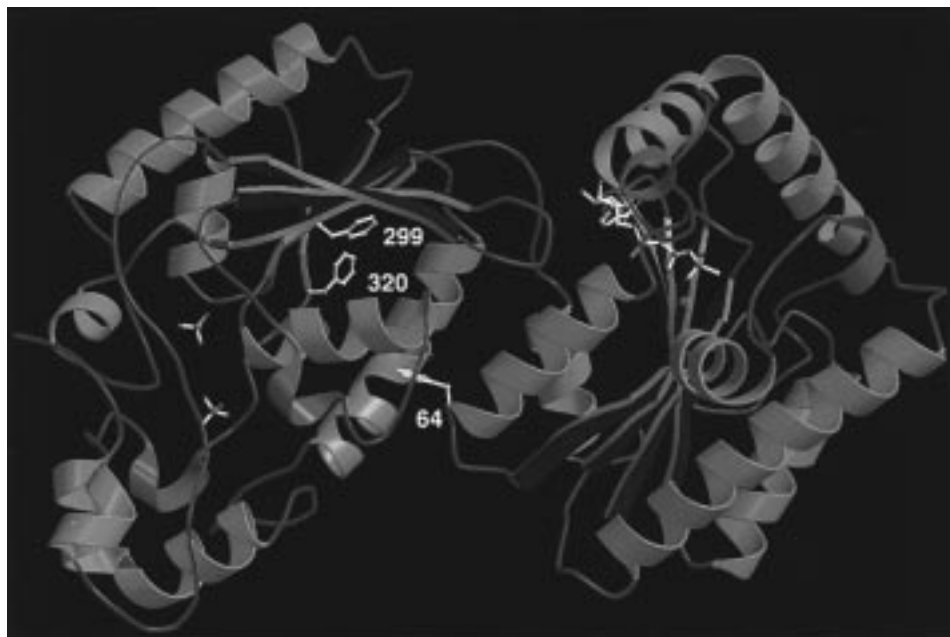


FIGURE 1: Crystal structure of fructose 6-phosphate,2-kinase/fructose 2,6-bisphosphatase showing locations for the three phenylalanine residues (64, 299, and 320) replaced with tryptophans in this study.

copy of a tryptophan residue contains contributions from the overall rotational diffusion of the protein (global motion) as well as from segmental motions of the tryptophan with respect to the rest of the protein (local motion). Assuming that the segmental motions occur independently of the overall protein rotation, the anisotropy decay, $r(t)$, is the product of separate processes (32, 36), and in the simplest, limiting case

$$r(t) = r_0[f_1 \exp(-t/\phi_1) + f_2 \exp(-t/\phi_2)] \quad (1)$$

where r_0 is the time zero anisotropy (the limiting anisotropy; fixed in our analysis to 0.305), t is the time after excitation, ϕ_1 and ϕ_2 are rotational correlation times (equal to the Debye rotational relaxation time divided by 3) associated with the "global" and "local" rotations, respectively, and f_1 and f_2 are the fractional changes in anisotropy associated with ϕ_1 and ϕ_2 , respectively. This equation was converted to the frequency domain by the method outlined by Weber (37), and fits were performed using a nonlinear least-squares analysis with software from ISS, Inc. (Champaign, IL). As with the lifetime analysis, frequency-independent standard deviations of 0.2° and 0.004 for phase and modulation, respectively, were used. The error analyses were performed as with the lifetime measurements.

Excitation polarization spectra and anisotropy ratios were obtained on an ISS PC, photon-counting spectrofluorimeter with the emission at $\lambda > 330$ nm viewed through a Corning 7-54 broad band-pass filter and a Schott WG335 cut-on filter. All measurements were done at 20 °C.

The fructose-6-P and fructose-2,6-P₂ titrations of the W15 mutant were carried out using an ISS K2 spectrofluorimeter with 300 nm excitation and with emission at $\lambda > 330$ nm viewed through a Corning 0-52 cut-on filter. For the fructose-6-P and fructose-2,6-P₂ titrations, the concentration of the W15 mutant was 9.1 and 2.0 μ M, respectively. The nonhydrolyzable ATP analogue, AMP-PNP, was added to 0.5 mM in separate titrations with fructose-6-P and fructose-2,6-P₂, but had no effect in either case. The additivity

property of anisotropy (38, 39) allows one to calculate the fraction of protein bound at each total ligand concentration via the following relation:

$$\text{Fraction bound} = \frac{(r_{\text{obs}} - r_{\text{free}})/(r_{\text{bound}} - r_{\text{free}}) + (g - 1)(r_{\text{bound}} - r_{\text{obs}})}{g} \quad (2)$$

where r_{obs} is the anisotropy observed at each ligand concentration, r_{free} is the anisotropy of W15 without ligand, r_{bound} is the anisotropy of W15 in the presence of a large excess of ligand, and g is the enhancement factor, that is, the ratio of the quantum yield of the fluorophore with and without ligand. The amount of bound ligand (the same as bound protein assuming 1:1 stoichiometry) is then the fraction bound times the total ligand concentration, and the concentration of free ligand is then the total ligand concentration minus the bound ligand concentration. In the case of W15, the fluorescence intensity did not vary significantly upon ligand binding (which was consistent with the very small change in the lifetime upon ligand binding), and hence, the enhancement factor was unity. The raw data was then plotted as fraction bound versus free ligand concentration, and the data were fit with the following hyperbolic function after Winzor and Sawyer (40).

$$\text{Fraction bound} = p[\text{Ligand}]_{\text{free}}/(K_d + [\text{Ligand}]_{\text{free}}) \quad (3)$$

where $[\text{Ligand}]_{\text{free}}$ is the free ligand concentration, p is the number of binding sites (fixed to one), and K_d is the dissociation constant given in the same units as the ligand concentration. Three or four titrations were performed for each ligand, and the weighted averages of the fitted values (K_d) are reported, plus or minus the weighted error.

RESULTS

The locations of the three phenylalanine residues which replace tryptophans 64, 299, and 320 are indicated in Figure 1. Lifetime data for each single-tryptophan mutant were

Table 1: Lifetimes of the Four Single-Tryptophan Mutants: Gaussian Distribution Model^a

protein	center (ns)	width (ns)	f_1	τ_2 (ns)	f_2	χ^2
W15	4.66 [± 0.02]	1.85 [$+0.03, -0.02$]	0.94	0.61 [$+0.01, -0.02$]	0.06	0.65
W15 + Fru-6-P ^b	4.87 [± 0.03]	1.13 [± 0.05]	0.96	0.85 [$+0.03, -0.04$]	0.04	0.53
W64	5.16 [± 0.02]	1.14 [± 0.03]	0.95	0.78 [± 0.02]	0.05	0.33
W299	6.73 [$+0.07, -0.06$]	1.70 [± 0.1]	0.96	0.76 [± 0.06]	0.04	3.5
W320	3.90 [$+0.00, -0.01$]	1.61 [± 0.01]	0.98	0.62 [± 0.02]	0.02	0.15

^a Center refers to the center value of the Gaussian distribution, width refers to the full-width at half-maximum for the distribution, f_1 and f_2 correspond to the fractional contributions to the intensity of the two lifetime components, and χ^2 is the reduced chi-square value corresponding to the fit of the phase and modulation data to the model. ^b 200 μ M fructose-6-P was added to the W15 mutant.

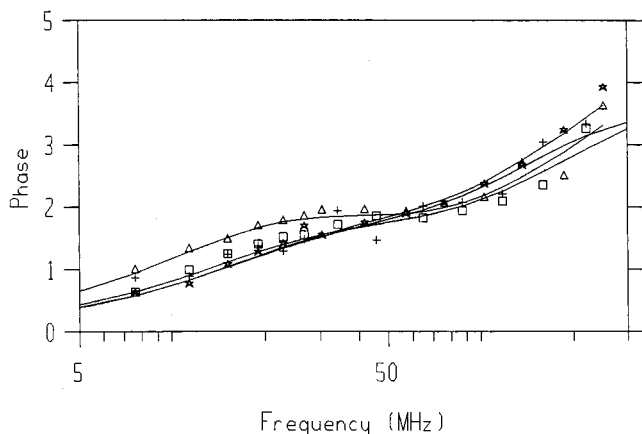


FIGURE 2: Dynamic polarization data of each single-tryptophan mutant. Differential phase angles (+, W15; □, W64; △, W299; and ★, W320) are plotted as a function of frequency, with the solid lines describing fits to the data. The values from the fits are summarized in Table 2.

Table 2: Dynamic Polarization Parameters for the Four Single Tryptophan Mutants

protein	ϕ_1 (ns)	f_1	ϕ_2 (ns)	f_2	χ^2
W15	93 [$+53, -27$]	0.829	0.43 [$+0.09, -0.08$]	0.171	1.8
W64	90 [$+30, -20$]	0.839	0.37 [$+0.07, -0.06$]	0.161	1.4
W299	87 [$+13, -10$]	0.810	0.28 [$+0.04, -0.03$]	0.190	0.68
W320	70 [$+17, -13$]	0.789	0.32 [$+0.04, -0.01$]	0.211	0.65

^a ϕ_1 and ϕ_2 represent rotational correlation times, f_1 and f_2 represent fraction anisotropies, and χ^2 is the reduced chi-square for the nonlinear least-squares fit of the phase and modulation data to the model. The limiting anisotropy was fixed at 0.305, but all other parameters were allowed to vary.

analyzed according to either discrete or distributional models. In all cases, the single Gaussian distribution model gave fits comparable to those of three discrete exponentials and superior to the single Lorentzian distribution model. The center lifetime values and widths of the distributions for the various mutants are given in Table 1. In all cases, the distributed component accounted for the majority (>94%) of the emission.

Dynamic polarization data for the four single-tryptophan mutants are shown in Figure 2. These data were analyzed according to a two-component model. The longer value (ϕ_1) and the shorter value (ϕ_2) shall be referred to as “global” and “local” rotational correlation times, respectively. The recovered rotational correlation times, their relative amplitudes, and the chi-square values are given in Table 2. The “global” rotational correlation times recovered ranged from around 70 to 93 ns. In all cases, the extent of local motion accounted for only 17–21% of the total anisotropy.

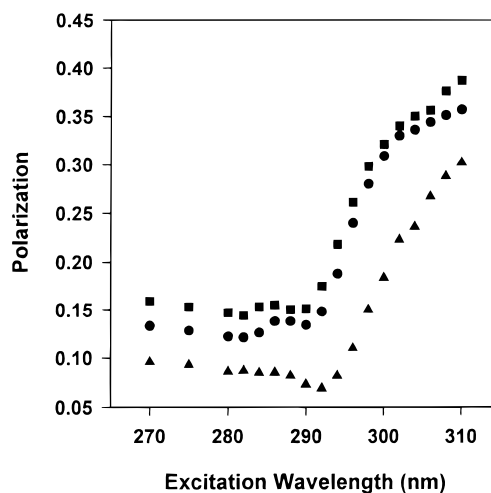


FIGURE 3: Excitation polarization spectra of W299 (●), W320 (■), and W299/W320 (▲), with emission > 320 nm.

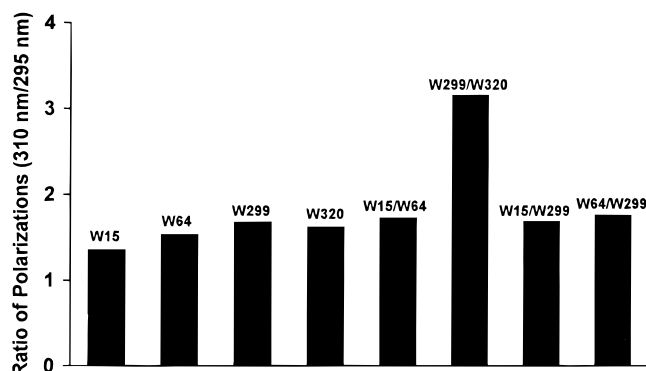


FIGURE 4: Ratios of polarizations (310/295) of various single- and double-tryptophan mutants.

The excitation polarization spectra associated with W299, W320, and W299/W320 at 20 °C are shown in Figure 3. Figure 4 gives the ratios of the polarizations observed for various proteins upon excitation at 310 and 295 nm, that is, the 310/295 ratio.

Direct-binding plots of fructose-6-P and fructose-2,6-P₂ are shown in Figure 5; the insets show the actual anisotropy data. The solid lines represent hyperbolic fits to the data points, from which dissociation constants were derived. The weighted averages of the dissociation constants are 29 ± 3 and $2.1 \pm 0.3 \mu$ M for fructose-6-P and fructose-2,6-P₂, respectively, as summarized in Table 3.

Figure 6 shows the dynamic polarization data for the W15 mutant in the absence and presence of 30 mM Fru-6-P. The marked difference between the two curves at high modulation frequencies is due to the decreased local mobility of the tryptophan residue in the presence of ligand. Without ligand,

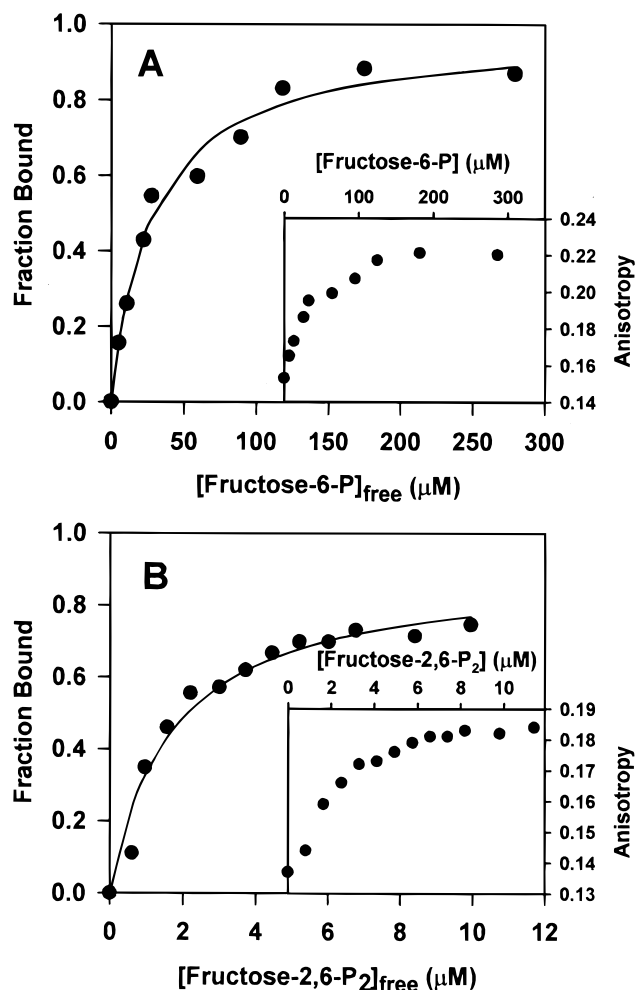


FIGURE 5: Examples of direct-binding plots of ligands to the W15 mutant. (A) Binding of fructose-6-P to 9.1 μM W15 mutant. (B) Binding of fructose-2,6- P_2 to 2 μM W15 mutant. The solid lines represent hyperbolic fits to the data. Derived dissociation constants are summarized in Table 3. Insets A and B show the raw anisotropy data.

Table 3: Dissociation Constants and Numbers of Binding Sites for Fructose-6-P and Fructose-2,6- P_2 ^a

ligand	K_d	K_M^b
fructose-6-P	$29 \pm 3 \mu\text{M}$	$50 \pm 10 \mu\text{M}$
fructose-2,6- P_2	$2.1 \pm 0.3 \mu\text{M}$	$41 \pm 14 \text{nM}$

^a Dissociation constants are derived from fits to the data from the direct-binding plots (Figure 5) as described in Materials and Methods: 1:1 binding was assumed in these calculations. ^b The values of K_M are from ref 14.

local mobility constitutes 17% ($\pm 1\%$) of the total motion, whereas the addition of 30 mM Fru-6-P decreases the local mobility to 2% ($\pm 1\%$) of the total motion. The decrease in local mobility upon addition of ligand thus accounts for the increase in anisotropy shown in Figure 5.

DISCUSSION

The crystal structure of fructose 6-phosphate,2-kinase/fructose 2,6-bisphosphatase was obtained using a mutation with all four tryptophan residues replaced by phenylalanines (13). This variant, however, and all of the single- and double-tryptophan variants employed in this study had very similar kinetic properties (K_m and V_{max}). The NH_2 -terminal

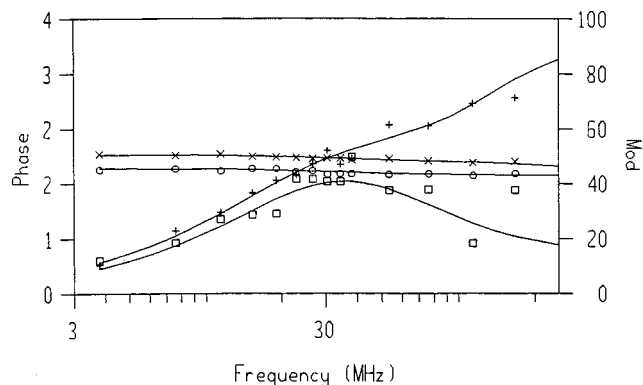


FIGURE 6: Dynamic polarization data of the W15 single mutant with and without fructose-6-P. The upper curves are the data for W15 alone (+, differential phase angle; \times , modulation ratio of perpendicular to parallel polarized component), and the lower curves are the data for W15 in the presence of 30 mM Fru-6-P (\square , differential phase angle; \circ , modulation ratio). Solid lines represent fits to the data.

36 amino acids were not visible in the electron density map which indicates that this portion of the enzyme is either highly mobile or disordered in the crystal lattice. The crystallographic temperature factors (B-factors) associated with the three resolved phenylalanine residues are 25 \AA^3 (F64), 29 \AA^3 (F299), and 22 \AA^3 (F320), while the average B-factor for the entire structure was 32 \AA^3 . These values are indicative of residues with limited mobilities. Our dynamic polarization data on the four tryptophan residues, however, demonstrate that all four residues have considerable local mobility suggesting that the limited mobilities of the phenylalanine residues in the crystal lattice do not represent the type of mobilities experienced by the tryptophan residues in the protein in solution. Whether these differences are due to the constraints of the crystal lattice per se or actually represent differences due to substitution of phenylalanine for tryptophan remains to be determined. The fact that the 36 N-terminal amino acid residues could not be resolved in the crystal structure coupled with the observation that all four tryptophans in the solution structure have similar mobilities also suggest that the dynamic properties of at least parts of the protein in the crystal lattice differ appreciably from those in solution. The lifetime data for the four single-tryptophan mutants were, in all cases, heterogeneous and could not be well fit to a single or double discrete exponential decay. Heterogeneous lifetimes for single-tryptophan proteins are, in fact, the rule rather than the exception (41–43). The excited-state kinetics of a number of single-tryptophan proteins have been analyzed in terms of continuous lifetime distribution models (33–35, 44, 45). The distributional approach to analyzing the excited-state kinetics of single-tryptophan proteins is based on the hypothesis that multiple interconvertible protein conformations exist and that the dynamics of the interconversion of the tryptophan residues between these substates affects the fluorescence lifetime (45). Distributional models are characterized by two parameters, namely, the center lifetime value and the width, that is, full width at half-maximum. Although none of the single-tryptophan mutant lifetime data could be reasonably fit with one or two discrete exponential decays, they all fit well to Gaussian distribution models with center lifetime values ranging from 3.90 ns (W320) to 6.73 ns (W299) (Table 1).

The dynamic polarization results on the single-tryptophan mutants indicated that each of these tryptophan residues exhibited local mobility which amounted to approximately 17–21% of the total anisotropy. Interestingly three of the “global” rotational correlation times recovered (W15, W64, W299) were very similar, namely 87–93 ns. For the W320 mutant, on the other hand, a rotational correlation time of 70 ns was recovered. These values may be compared to the global rotational correlation time of ~60 ns determined for the protein using the covalently attached, sulfhydryl specific probe AEDANS (46). As pointed out previously in that study, a spherical macromolecule of 110 kDa would be expected to exhibit a rotational correlation time in the range of 40–50 ns depending upon the partial specific volume and extent of hydration; the AEDANS data thus provided early evidence that the protein was nonspherical. The recently published crystal structure supported this conclusion and indicated that the protein (in the crystal lattice) is, in fact, asymmetric with an axial ratio of approximately 2:1. The observed range of rotational correlation times from the various probes (60 ns from AEDANS and 70–93 ns from the tryptophan residues) is entirely consistent with such an elongated molecule. The experimentally determined rotational correlation times depend on the orientation of the excitation and emission dipoles of the probes with respect to the principle rotational axes of the macromolecule (47, 48), and observed differences in rotational rates among the various tryptophan residues and the AEDANS probe presumably reflect these orientational differences. We must also note, however, that large uncertainties are associated with the recovered correlation times (Table 2) of the tryptophan data which reflect the relatively short lifetimes of the tryptophan residues compared to the global rotational rate.

The steady-state anisotropies and lifetimes of W64, W299, and W320 are not influenced by the presence of fructose-6-P (data not shown). On the other hand, the anisotropy of the W15 mutant, upon 300 nm excitation, is significantly affected by both fructose-6-P and fructose-2,6-P₂. The increase in anisotropy upon binding of either ligand to the protein can be used to generate a binding isotherm (Figure 5) and to provide an estimate of the dissociation constant for the protein/ligand complex. These data are significant, not only since they provide direct information on the dissociation constant of these ligands, but also because only W15 was significantly affected upon binding of these ligands, suggesting either that the binding sites are in the vicinity of tryptophan 15 or that they can influence this region of the protein when bound. Moreover, the data suggest that fructose-2,6-P₂ binds to the kinase site in the N-terminus in addition to any other sites, that is, the phosphatase site in the C-terminus. Binding at the kinase site may explain the difference between the dissociation constant reported here (2 μM) and the K_M value (41 nM) reported previously (14) and the relative agreement between K_d and K_M for fructose-6-P (29 versus 50 μM, respectively). We note that fructose-2,6-P₂ also increases the anisotropy of W299 upon binding and suggests a submicromolar dissociation constant (data not shown), more consistent with the reported K_M of 41 nM. The change in anisotropy of W299 upon fructose-2,6-P₂ binding is smaller than that of W15, making data analysis more difficult.

The increase in anisotropy of W15 could, in principle, be due to either a decrease in the fluorescence lifetime upon ligand binding or a decrease in the rotational mobility of W15 in the presence of bound ligand. In fact, the center value of the lifetime for W15 is not changed significantly in the presence of saturating levels of fructose-6-P (Table 1), whereas the width of the recovered Gaussian distribution is decreased in the presence of fructose-6-P. Changes in the widths of lifetime distributions of tryptophan residues have been attributed to changes in interconversion rates between protein conformers (in temperature or denaturation studies) or to changes in the number of protein environments available (in cases of added ligands) (33–35, 44, 45). In this case, the dynamic polarization data (Figure 6) demonstrates that the local mobility of W15 is significantly reduced in the presence of Fru-6-P (from 17% (±1%) to 2% (±1%)). Hence, the decrease in the width of the lifetime distribution in the presence of ligand indicates that ligand binding reduces the motion of W15 and consequently restricts the number of protein environments accessible to the excited fluorophore. The increased anisotropy of W15 upon ligand binding is thus due to the almost complete disappearance of its local mobility. These results provide direct physical evidence that the N-terminal peptide of the bifunctional enzyme may be bound to the surface of the catalytic domains in the presence of Fru-6-P, perhaps near the kinase active site, but is highly mobile in the absence of the substrate. This observation is the first demonstration of ligand-induced conformational changes mediated by enhanced interaction of the N-terminal peptide of Fru-6-P,2-kinase/Fru-2,6-bisphosphatase. Previous studies had provided only indirect evidence such as Fru-6-P-induced protection of the bifunctional enzyme against inactivation by heat, denaturants, or protein-concentration-dependent dissociation (15).

The N-terminus is significant because it has been suggested to play roles in subunit interaction and in both catalytic activities. In a previous study where 24–30 of the N-terminal residues were deleted, the K_M for Fru-6-P greatly increased, the kinase activity decreased, and the phosphatase activity increased (15). Moreover, these deletion mutants were more susceptible to protein-concentration-dependent dissociation and thermal inactivation, while binding of Fru-6-P protected against thermal inactivation. Introduction of a phosphorylation site (a serine residue) at position 30 of the testis enzyme and subsequent phosphorylation by protein kinase A resulted in inhibition of the kinase by increasing the K_M for Fru-6-P, as well as activation of the phosphatase activity (49). Also, the phosphoenzyme was more susceptible to thermal and urea inactivation. These results led us to suggest that the N-terminus is essential in stabilizing the dimer structure, perhaps involved in the subunit–subunit interaction (15). The dimeric structure of the Fru-6-P,2-kinase domains is apparent in the crystal structure (13) where the subunits interact to form a continuous, 12-stranded intermonomer β shunt.

Weber (50) had measured the excitation polarization spectrum for the aromatic amino acids and several proteins and had demonstrated that tyrosine to tryptophan energy transfer in proteins could be detected by measuring the ratio of the polarizations observed upon excitation at 305 and 275 nm (the 305:275 ratio). He also demonstrated that tryptophan to tryptophan energy transfer occurred in concentrated

solutions of indole, but that the transfer efficiency diminished as the excitation wavelength approached the red edge of the excitation spectrum. This "red-edge" effect was observed to be a general phenomenon characterizing energy transfer between identical molecules at the long wave edge of the absorption spectrum (51). Depolarization between tryptophan residues in ditryptophan and polytryptophan and failure of energy transfer at the red edge in these systems was also reported by Weber and Shinitzky (51). Their data indicated that the ratio of the polarizations observed upon excitation at 310 and 295 nm, the 310:295 ratio, provides an indication of the extent of energy transfer since the 295 value is directly affected by the efficiency of self-transfer, while the 310 value is significantly less affected due to the failure of self-transfer at the excitation red-edge. We have utilized this red-edge phenomenon to study energy transfer between tryptophan residues in the various double-tryptophan mutants. As shown in Figure 4, the 310:295 ratio is in the range of 1.3–1.7 for all single-tryptophan mutants as well as for the double-tryptophan mutants W15/64, W15/299, and W64/299. However, this ratio was significantly increased (>3) in the case of W299/320. Figure 3 shows the complete excitation polarization spectrum for the W299, W320, and W299/W320 mutants. We conclude that residues W299 and W320 can efficiently transfer excitation energy and hence are in close proximity in the protein. W15, however, is not able to transfer to W64 or W299 suggesting that these positions in the protein structure are not in close proximity. The crystal structure, in fact, indicates that positions W299 and W320 (or more correctly the phenylalanine residues which replace these tryptophans in the crystallized material) are ~5 Å apart; since W15 does not appear in the crystal structure, however, we cannot correlate the solution results with the X-ray data. Our previous observation (vide supra), though, that the polarization of the wild-type protein was lower than that observed for any single-tryptophan mutants can be attributed to energy transfer between W299 and W320.

ACKNOWLEDGMENT

We acknowledge Cu Nguyen and Yang Li (Dallas, TX) for expression and purification of the proteins. The time-resolved fluorescence measurements were done at the Laboratory for Fluorescence Dynamics at the University of Illinois, Urbana–Champaign, which is supported by the National Institutes of Health (RR03155).

REFERENCES

- Uyeda, K. (1991) in *A Study of Enzymes: CRC Review* (Kuby, S. A., Ed.) Vol. II, pp 445–456, CRC Press, Boston, MA.
- Rider, M. H., Marchand, M. J., Hue, L., and Rousseau, G. G. (1987) *FEBS Lett.* 224, 317–321.
- Algaier, J., and Uyeda, K. (1988) *Biochem. Biophys. Res. Commun.* 153, 328–333.
- Lively, M. O., el-Maghrabi, M. R., Pilkis, J., D'Angelo, G., Colosia, A. D., Ciavola, J. A., Fraser, B. A., and Pilkis, S. J. (1988) *J. Biol. Chem.* 263, 839–849.
- Crepin, K. M., Darville, M. I., Michel, A., Hue, L., and Rousseau, G. G. (1989) *Biochem. J.* 264, 151–160.
- Sakata, J., and Uyeda, K. (1990) *Proc. Natl. Acad. Sci. U.S.A.* 87, 4951–4955.
- Sakata, J., Abe, Y., and Uyeda, K. (1991) *J. Biol. Chem.* 266, 15764–15770.
- Van Schaftingen, E., Davies, D. R., and Hers, H. G. (1981) *Biochem. Biophys. Res. Commun.* 103, 362–368.
- el-Maghrabi, M. R., Claus, T. H., Pilkis, J., and Pilkis, S. J. (1982) *Proc. Natl. Acad. Sci. U.S.A.* 79, 315–319.
- Furuya, E., Yokoyama, M., and Uyeda, K. (1982) *Proc. Natl. Acad. Sci. U.S.A.* 79, 325–329.
- Kitamura, K., and Uyeda, K. (1987) *J. Biol. Chem.* 262, 679–681.
- Kitamura, K., Uyeda, K., Kangawa, K., and Matsuo, H. (1989) *J. Biol. Chem.* 264, 9799–9806.
- Hasemann, C. A., Istvan, E. S., Uyeda, K., and Deisenhofer, J. (1996) *Structure* 4, 1017–1029.
- Watanabe, F., Jameson, D. M., and Uyeda, K. (1996) *Protein Sci.* 5, 904–913.
- Tominaga, N., Minami, Y., Sakakibara, R., and Uyeda, K. (1993) *J. Biol. Chem.* 268, 15951–15957.
- Kurland, I. J., Li, L., Lange, A. J., Correia, J. J., el-Maghrabi, M. R., and Pilkis, S. J. (1993) *J. Biol. Chem.* 268, 14056–14064.
- Barry, J. K., and Matthews, K. S. (1997) *Biochemistry* 36, 15632–15642.
- Dijkstra, D. S., Broos, J., Visser, A. J., van Hoek, A., and Robillard, G. T. (1997) *Biochemistry* 36, 4860–4866.
- Graether, S. P., Heinonen, T. Y., Raharjo, W. H., Jin, J. P., and Mak, A. S. (1997) *Biochemistry* 36, 364–369.
- Hennecke, J., Sillen, A., Huber-Wunderlich, M., Engelborghs, Y., and Glockshuber, R. (1997) *Biochemistry* 36, 6391–6400.
- Ionescu, R. M., and Eftink, M. R. (1997) *Biochemistry* 36, 1129–1140.
- Jonasson, P., Aronsson, G., Carlson, U., and Jonsson, B. H. (1997) *Biochemistry* 36, 5142–5148.
- Nath, U., and Udgaonkar, J. B. (1997) *Biochemistry* 36, 8602–8610.
- Wang, Q., Matsushita, K., de Foresta, B., le Maire, M., and Kaback, H. R. (1997) *Biochemistry* 36, 14120–14127.
- Bradford, M. M. (1976) *Anal. Biochem.* 72, 248–254.
- Sakakibara, R., Tanaka, T., Uyeda, K., Richards, E. G., Thomas, H., Kangawa, K., and Matsuo, E. (1985) *Biochemistry* 24, 6818–6824.
- Gratton, E., Jameson, D. M., Rosato, N., and Weber, G. (1984) *Rev. Sci. Instrum.* 55, 486–494.
- Alcala, J. R., Gratton, E., and Jameson, D. M. (1985) *Anal. Instrum.* 14, 225–250.
- Spencer, R. D., and Weber, G. (1970) *J. Chem. Phys.* 52, 1654–1660.
- Spencer, R. D., and Weber, G. (1969) *Ann. N.Y. Acad. Sci.* 158, 361–376.
- Jameson, D. M., Gratton, E., and Hall, R. D. (1984) *Appl. Spectrosc. Rev.* 20, 55–106.
- Jameson, D. M., and Hazlett, T. L. (1991) in *Biophysical and Biochemical Aspects of Fluorescence Spectroscopy* (Dewey, G., Ed.) pp 105–133, Plenum Press, New York, NY.
- Alcala, J. R., Gratton, E., and Prendergast, F. G. (1987) *Biophys. J.* 51, 587–596.
- Alcala, J. R., Gratton, E., and Prendergast, F. G. (1987) *Biophys. J.* 51, 596–604.
- Alcala, J. R., Gratton, E., and Prendergast, F. G. (1987) *Biophys. J.* 51, 925–936.
- Gratton, E., Jameson, D. M., and Hall, R. D. (1984) *Annu. Rev. Biophys. Bioeng.* 13, 105–124.
- Weber, G. (1977) *J. Chem. Phys.* 66, 4081–4091.
- Weber, G. (1952) *Biochem. J.* 51, 145–155.
- Jameson, D. M., and Sawyer, W. H. (1995) *Methods Enzymol.* 246, 283–300.
- Winzor, D. M., and Sawyer, W. H. (1995) *Quantitative Characterization of Ligand Binding*, Wiley-Liss, New York.
- Beechem, J. M., and Brand, L. (1985) *Annu. Rev. Biochem.* 53, 43–71.
- Eftink, M. R. (1991) in *Methods of Biochemical Analysis* (Suelter, C. H., Ed.) pp 127–205, John Wiley & Sons, New York.

43. Demchenko, A. P. (1992) in *Topics in Fluorescence Spectroscopy* (Lakowicz, J. R., Ed.) pp 65–111, Plenum Press, New York.
44. Gratton, E., Silva, N., Mei, G., Rosato, N., Savini, I., and Finazzi-Agro, A. (1992) *Int. J. Quantum Chem.* 42, 1479–1489.
45. Silva, N., Mei, G., and Gratton, E. (1994) *Comm. Mol. Cell. Biophys.* 8, 217–242.
46. Tominaga, N., Jameson, D. M., and Uyeda, K. (1994) *Protein Sci.* 3, 1245–1252.
47. Beechem, J. M., Knutson, J. R., and Brand, L. (1986) *Biochem. Soc. Trans.* 14, 832–836.
48. Brunet, J. E., Vargas, V., Gratton, E., and Jameson, D. M. (1994) *Biophys. J.* 66, 446–453.
49. Abe Y., and Uyeda, K. (1994) *Biochemistry* 33, 5766–5771.
50. Weber, G. (1960) *Biochem. J.* 75, 335–345.
51. Weber, G., and Shinitzky, M. (1970) *Proc. Natl. Acad. Sci. U.S.A.* 65, 823–830.

BI980202W